

Co-published by Institute of Fluid-Flow Machinery Polish Academy of Sciences

Committee on Thermodynamics and Combustion

Polish Academy of Sciences

Copyright@2025 by the Authors under licence CC BY-NC-ND 4.0

http://www.imp.gda.pl/archives-of-thermodynamics/



Analysis of the feasibility of using Invar process pipes in multichannel cryogenic helium transfer lines based on the second law of thermodynamics

Pawel Duda*, Maciej Chorowski, Ziemowit Malecha, Jarosław Poliński

Wrocław University of Science and Technology, Wybrzeże Stanisława Wyspiańskiego 27, 50-370 Wrocław, Poland *Corresponding author email: pawel.duda@pwr.edu.pl

Received: 29.12.2024; revised: 20.02.2025; accepted: 21.02.2025

Abstract

This work describes examples of the use of cryogenic lines and their designs, referring in detail to typical structural nodes found in cryogenic transfer lines. As a special case, multichannel cryogenic transfer lines are described, in which the process pipes are made of Invar. This has a significant impact on the number of internal supports and the method of thermal shrinkage compensation, which directly impact into reduced heat input during the transfer of cryogenic media. The second law of thermodynamics and the Gouy-Stodola theorem are discussed from the perspective of their application in optimizing and evaluating heat and mass transfer devices. The next part of the work presents the internal structure of the selected 250 m multichannel cryogenic transfer line. Several variants of the method of supporting process pipes have been presented and compared with the solution using Invar. For each solution, an entropy analysis was carried out in order to select the best design in terms of the entropy generated in the process pipes. From the examples presented, it is proven that entropy minimization method can be used for complex optimization of entire cryogenic distribution systems, as well as their individual components.

Keywords: Cryogenic; Cryogenic lines; Entropy minimization; Invar

Vol. 46(2025), No. 4, 5-13; doi: 10.24425/ather.2025.154196

Cite this manuscript as: Duda, P., Chorowski, M., Malecha, Z., & Poliński, J. (2025). Analysis of the feasibility of using Invar process pipes in multichannel cryogenic helium transfer lines based on the second law of thermodynamics. *Archives of Thermodynamics*, 46(2), 5–13.

1. Introduction

Big Science research infrastructure, like particle accelerators, free electron lasers, tokamaks and other machines, makes an extensive use of helium cryogenics, allowing a stable operation of superconducting magnets and superconducting radio frequency cavities in temperatures as low as 1.8 K (superfluid helium). Cold helium, in most cases in a supercritical thermodynamic state, is transferred from the helium refrigerator to the cryomodules comprising the magnets and the cavities with the use of cryogenic distribution systems (CDS). Cryogenic distribution systems typically consist of multichannel cryogenic cold helium transfer lines and so-called valve boxes interconnecting the transfer line with the cryostats.

The role of cryogenic transfer lines is not only to supply cold helium to the valve boxes, but also to recover and transfer to the cryoplant cold helium vapours leaving the cryomodules. In most cases, the multichannel helium cryogenic transfer lines comprise four process lines: supercritical helium supply line, cold helium vapours return line, thermal shield cooling inlet line and thermal shield cooling outlet line. All the process lines are located in the vacuum vessel and are surrounded by an actively cooled thermal shield. This, along with a multilayer insulation (MLI) covering the process lines and thermal shield, constitutes highly effective thermal insulation of the process lines, which is essential for the proper operation of any cryogenic helium device [1]. Exemplary

Nomenclature

d – inside diameter, m

D – outside diameter, m

E - Young's Modulus, GPa

f – pipe deflection, m

g – gravitational acceleration, m²/s

L – length of the pipe, m

 \dot{n} – mass flow rate, kg/s

P – power, W

p - pressure, Pa

q − heat flux, W

 \dot{S} – entropy flux, W/K

T - temperature, K

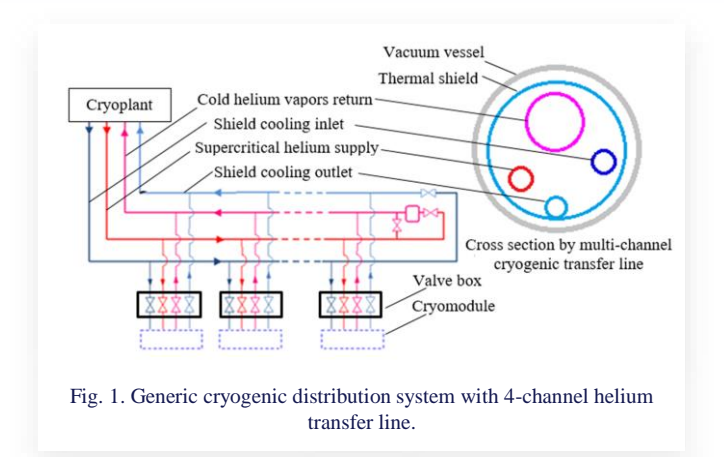
w - medium flow velocity, m/s

a – allowable distance between sliding supports, m

Greek symbols

Δ − difference

λ – flow coefficient (Darcy friction factor)



cross-section of 4-channel helium transfer line is depicted in Fig. 1.

Due to the huge size of research facilities, such as the Large Hadron Collider (LHC), the planned Future Circular Collider (FCC) at CERN (*Conseil Européen pour la Recherche Nucléaire*) or the International Thermonuclear Experimental Reactor (ITER), it is necessary to transfer cryogenic fluids over considerable distances to cool superconducting elements [2–4].

The length of multichannel helium transfer lines may differ from tens meters to several kilometers. They may be located in outer space or in deep underground accelerator tunnels. The longest single multichannel helium transfer line is used for suppling the Large Hadron Collider magnets along one sector of the machine at the distance of 3.3 km [5].

The specific power of cryogenic refrigerators, defined as the power requirement at 300 K to produce one watt of cooling power at 4.5 K, is currently around 220 W [6]. This results from the fact that in an ideal, Carnot cycle the 1 watt of cooling power at 4.5 K temperature requires minimum 65 W of electric power, while today's state-of-art helium refrigerators are characterized by thermodynamic efficiencies in the range of 30–40% of Car-

 ζ – local pressure loss coefficient

 ρ – density, kg/m³

 Σ – sum

Subscripts and Superscripts

4 – ambient

C - cryogen

INV - Invar

He - helium

in - input value

out - output value

Abbreviations and Acronyms

AMTF – accelerator module test facility

DESY - Deutsches Elektronen Synchrotron

FCC - Future Circular Collider

XATL – cryogenic transfer line for supercritical helium transport from the Hadron-Electron Ring Accelerator refrigerator to accelerator module test facility hall

XFEL - X-Ray Free Electron Laser

not cycle efficiency [7,8]. This means that even a slight reduction in heat input to the cryogenic medium during its transfer to the cryostats has a huge impact on reducing the power needed to drive the cryogenic refrigerator, thus, on reducing the energy consumption of the entire research device. The radiation and convection heat transfer to the process pipes can be reduced to almost negligible values by the use of insulation vacuum and multilayer insulation [9]. What is very difficult to be avoided are heat fluxes conducted by material of the mechanical internal supports of the process lines that constitute the thermal bridges between the room and process lines temperatures, and which in the cryogenic transfer line design cannot be avoided. On the other hand, the supports are the elements of the transfer lines characterized by the greatest repeatability in the entire structure. Therefore, thermal optimization of supports, or limiting their number, effectively affects the significant improvement of the thermal efficiency of the entire transfer line.

From a novelty perspective, the impact of using Invar process pipes on the mechanical, thermal, and hydraulic properties of the pipeline has been examined. By applying the entropy generation minimization method, the effect of using Invar process pipes and a new support system has been distilled into a clear and quantifiable parameter for engineers. This parameter represents the actual additional power required to compensate for the irreversibilities occurring in pipelines with the tested thermal and structural properties.

Entropy generation is a fundamental concept in thermodynamics and statistical mechanics, playing a pivotal role in understanding the behaviour of various physical systems. It provides critical insights into the irreversibility and inefficiency of processes and is intrinsically linked to the second law of thermodynamics. According to this law, the entropy of a system increases over time. Irreversibilities in physical processes lead to the generation of entropy. The concept of entropy generation has numerous applications across fields such as chemistry, biology, engineering, and environmental science. The optimization of

process efficiency and the minimization of energy losses have prompted extensive investigation into entropy generation by engineers and scientists [10]. Khan et al. [11] applied the second law of thermodynamics to determine the total entropy rate, considering three distinct forms of irreversibility: heat transfer, fluid friction, and the Darcy-Forchheimer relation. Mohanty et al. [12] examined the effects of entropy production on the peristaltic transport of micropolar nanofluids. Nadeem [13] conducted research on entropy analysis in the stagnation-point flow of a hybrid nanofluid. The variation in fluid properties was investigated in terms of the velocity field, entropy generation, and induced magnetic field, with respect to the mixed convection parameter.

By employing optimization methods based on the second law of thermodynamics, it is possible to account for thermal processes, flow processes, and design parameters that describe the optimized system. The primary advantage of the described method lies in its ability to simultaneously consider multiple physical parameters that characterize various thermodynamic and mechanical states. However, a potential disadvantage is that the optimization results, which indicate the entropy generation rate, may be challenging for engineers to intuitively interpret. This contrasts with thermal or flow optimizations, where the outcomes are typically represented by measurable quantities such as heat flux or pressure drop. In such cases, the Gouy-Stodola theorem and the real efficiency of thermal-flow machines provide valuable insight. By using the entropy generation rate, these concepts enable the determination of the theoretical and real additional power required for the operation of the analysed system. The real additional power, necessary to overcome the irreversibilities present in the system, represents a clear and practical parameter for engineers.

2. Methodology based on second law of thermodynamics

The second law of thermodynamics implies that during each irreversible process, the sum of entropy of the system and its surroundings increases. For an integrated entropy generation, additional power necessary to overcome the irreversibilities accompanying the flow of cryogen in the transfer pipes, can be calculated from the Gouy-Stodola theorem described by the following equation [14,15]:

$$P_{Ad} = T_A \dot{S},\tag{1}$$

where: P_{Ad} – additional power necessary to overcome the irreversibilities, T_A – ambient temperature, \dot{S} – entropy flux.

Equation (1) suggests that thermal objects should demonstrate possibly low entropy flux increases, especially in the processes of heat exchange and medium transfer. In cryogenic transfer lines, entropy increase is caused by two processes: pressure drop of the medium in the process pipe and heat exchange due to temperature difference between the cryogen and the surroundings [16]:

$$\dot{S} = \sum_{i} \dot{S}_{\Delta T} + \sum_{i} \dot{S}_{\Delta p},\tag{2}$$

where $\sum_i \dot{S}_{\Delta T}$ is the sum of entropy fluxes generated due to temperature differences and $\sum_j \dot{S}_{\Delta p}$ is the sum of entropy fluxes generated due to pressure drops in the pipeline. The processes of entropy generation in the process pipe of a cryogenic transfer line are shown in Fig. 2.

Entropy increase due to heat transfer can be calculated using the following formula:

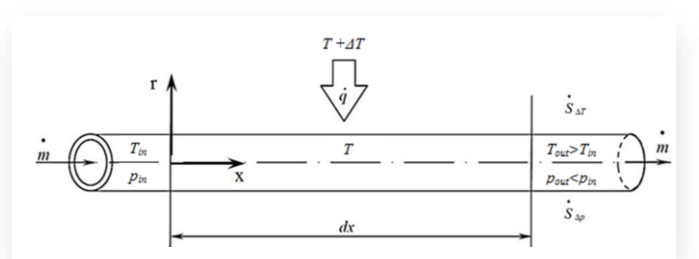


Fig. 2. Processes of entropy increase in a pipeline segment having length dx; \dot{m} – mass flow rate of the transferred medium, \dot{q} – heat flux, T – temperature of the medium, $T+\Delta T$ – ambient temperature, p – pressure, indexes in – input value, out – output value [14].

$$\dot{S}_{\Delta T} = \frac{\dot{q}}{T} - \frac{\dot{q}}{T + \Delta T}.\tag{3}$$

The second entropy source is pressure drop caused by local and linear flow resistivities described as

$$\dot{S}_{\Delta p} = \frac{\dot{m}}{\rho T} \Delta p = \frac{\dot{m} w^2}{2T} \left(\lambda \frac{L}{d} + \sum_n \zeta_n \right), \tag{4}$$

where: ρ – density of medium, Δp – pressure drops in the pipeline, w – medium flow velocity, λ – flow coefficient (Darcy friction factor), L – length of the pipe, d – diameter of the pipe, $\Sigma_n \zeta_n$ – the sum of local pressure loss coefficient.

The entropy production is increasing with the decrease of the process pipe temperature, which makes this entropy source especially important in cryogenic conditions. Equation (3) takes a special form for cryogenic liquid transfer:

$$\dot{S}_{\Delta T} = \frac{\dot{q}\Delta T}{T_C^2 \left(1 + \frac{\Delta T}{T_C}\right)},\tag{5}$$

where $\Delta T = T_A - T_C$, and T_C is the cryogen temperature.

This paper employs entropy analysis to compare three cryogenic lines of identical length, diameter of process pipes, and flow rates of the cryogen. Consequently, the entropy fluxes generated due to flow resistance are equivalent across all cases. The differences in entropy fluxes generated by heat leaks by process pipe support systems can be attributed to the materials used and the configuration of the pipe supports.

3. Process pipes support systems in multichannel cryogenic transfer line

In every multichannel cryogenic transfer line, several fundamental types of supports for process pipes are present. A generic schematic of a 250-meter section of the transfer line, along with all types of process pipe supports, is presented in Fig. 3. The pipeline is divided into 12-meter modules, which facilitate trans-

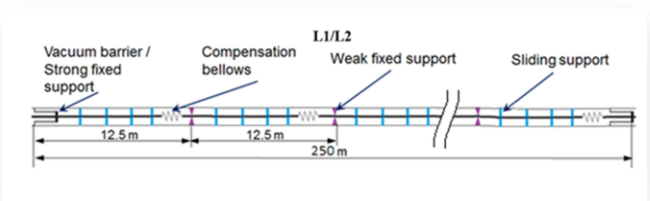


Fig. 3. The support systems for the process pipes of the typical multi-channel cryogenic transfer line.

portation. Each module is equipped with expansion bellows that mitigate the increase in stresses generated by the thermal contraction of the process pipes. The reduction of stresses resulting from thermal contraction, achieved through the use of expansion joints, is currently the most common method of compensation employed in cryogenic transfer lines. This approach necessitates the use of all the types of process pipe supports described below.

The most frequently recurring support in a cryogenic line is the sliding support. The purpose of the sliding support is to determine the vertical position of the process pipes while allowing them to move axially relative to each other and to the thermal shield [17]. In addition to sliding supports, there are two types of fixed supports. The 'strong' fixed support is designed to transfer relatively large forces generated by the compensation bellows, which are subjected to the pressure of the flowing cryogenic medium and is usually installed at the ends of a given section consisting of multiple straight section modules. The 'weak' fixed support is installed in each transfer line module that contains compensation bellows, and its task is to determine the radial and axial position of the process pipes, ensuring the correct operation of the bellows.

The use of compensation bellows implies the application of an appropriate support scheme to ensure bellows mechanical stability. This system requires the fix support on one side of the bellows and 4 sliding supports on the other side, all at a distance no larger than that specified by the bellows manufacturer. Therefore, regardless of the transfer line module length (distance between the individual fixed supports), transfer lines containing compensation bellows must include sliding supports for the process pipes.

The situation will be different for transfer lines, where the process lines are made of Invar. Due to one order of magnitude lower thermal expansion of Invar than stainless steel [18], in this case, the process lines do not require bellows to compensate for thermal shrinkage. This allows for the elimination of expansion bellows and weak fixed supports throughout the analysed structure, as presented in Fig. 4. In addition, the sliding supports between the strong supports are needed only for preventing the process line against the self-weight slanging. What is more, the

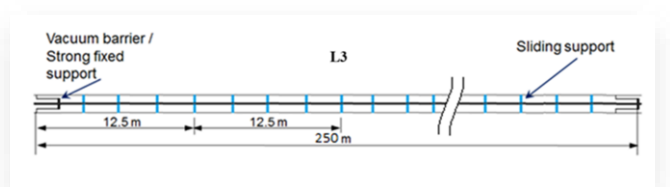


Fig. 4. The support systems for the process pipes for the case L3.

lack of the bellows further reduces system energy loses related with fluid flow pressure drop.

4. Case study

Three 250 m long straight segments of multichannel transfer lines L1, L2 and L3 were compared in order to examine how changing the support systems for process pipes influences the entropy fluxes generated in the process pipes and the additional power required to overcome the irreversibilities, which accompany the cryogen flow. Table 1 presents the geometric and thermodynamic parameters of the process pipes taken into account during the subsequent considerations in this paper.

Table 1. Operating parameters of transfer lines L1–L3.

		Operating parameters				
Process line	Dimension	<i>p,</i> MPa	T, K	<i>ṁ,</i> kg/s		
Supercritical helium supply '5 K'	Ø60.3 × 2	0.35	5.0	0.015		
Cold helium vapours return '4.5 K'	Ø88.9 × 2.3	0.12	4.5	0.015		
Thermal shield cooling inlet '45 K'	Ø48.3 × 2	1.70	45.0	0.010		
Thermal shield cool- ing outlet '60 K'	Ø48.3 × 2	1.67	60.0	0.010		

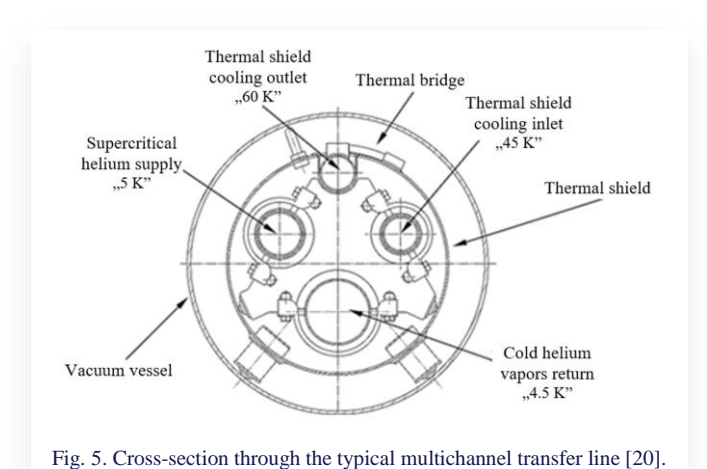
As shown in Table 1, in one multichannel line, a cryogenic medium with different thermodynamic parameters is transported through the process pipes – the supply pipe carries high-pressure supercritical helium, and the return pipe carries a gaseous or two-phase medium with low pressure. Additionally, a gaseous helium with a higher temperature range is sent through the pipe used to cool the thermal shields [19].

The support systems for the process pipes of the tested multichannel transfer lines sections for cases L1 and L2 are schematically shown in Fig. 3. The arrangement of sliding supports in the case of L2 is the same as in the case of L1. The only difference is the functional separation of one sliding support used in the case of L1 into three independent supports. The third case under consideration uses the same sliding supports as described for case L2, however the process pipes are made of Invar.

4.1. Cryogenic line using a standard type of sliding supports – L1

The first analysed case L1 is a standard solution based on the cross section of cryogenic transfer line (XATL1) used to supply helium to devices located in the accelerator module test facility (AMTF) hall for the European X-ray free electron laser (XFEL) accelerator operating at the Deutsches Elektronen Synchrotron (DESY) research centre in Hamburg (see Fig. 5). The geometric parameters of the described line were used as a starting point for optimization based on the method of minimizing the entropy generated.

Figure 5 shows a sliding support of the XATL1 that mechanically connects three process pipes: 5 K supply, 4.5 K return and 45 K inlet. This support rests on a thermal shield with a temperature of 60 K.



The presented solution allows for easy assembly of the transfer line and using only one design type of sliding support to support all process pipes. The disadvantage of this solution is the thermal connection of process lines with different temperatures, which results in an undesirable heat flow between the lines.

As already mentioned, in addition to sliding supports, there are two types of fixed supports in cryogenic lines. The geometry of the weak and strong fixed support used in the described analysis is shown in Figs. 6 and 7, respectively.

As it turns out, the method of supporting the process lines and, in particular, which process lines will be supported by a common support, have a very significant impact on the thermal efficiency of the cryogenic transfer line [21].

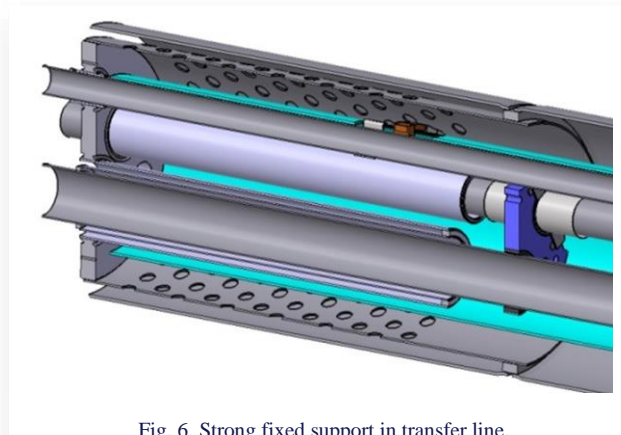


Fig. 6. Strong fixed support in transfer line.

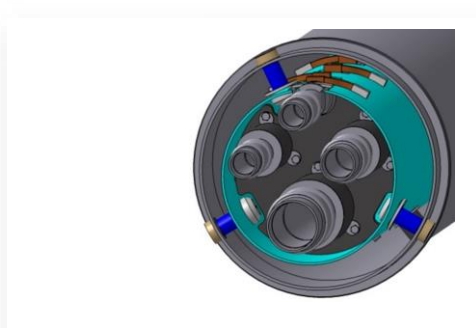
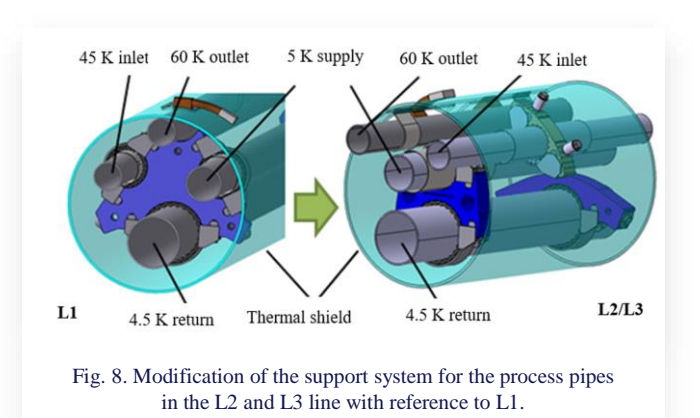


Fig. 7. Weak fixed support in transfer line.

4.2. Cryogenic line using a new type of sliding supports – L2

In order to avoid any unwanted thermal contacts in the sliding supports of the L2 line, additional types of supports were designed, as shown in Fig. 8, L2/L3 case. In this solution, the 45 K inlet line has separate, low heat-conduction support that is attached to the thermal shield. This eliminates heat flow from 45 K line to the 5 K supply line, as it is in the L1 case.



Another solution that thermally improves the sliding support system for the process lines is to use the support for the 5 K supply and 4.5 K vapour return lines only. In this case, the 4.5 K line acts as the mechanical support for the 5 K line and is sliding supported at a different location on the thermal shield. In such solution, there is almost no heat conduction between the 5 K and 4.5 K lines through the common sliding support, because the temperature difference is negligible and the support material has low thermal conductivity. Reduction of heat fluxes to the supply pipes allows reductions in the amounts of helium flowing, entails compensations of lower heat fluxes and thus offers a possibility to use smaller-diameter process pipes, to which less heat flows by radiation.

5. Results and discussion

5.1. Calculations of entropy 888fluxes generated in transfer line L1

In order to identify heat fluxes to the particular process pipes and to determine the resultant entropy fluxes, each support was subjected to thermal analysis. Each element of the model was assigned material properties, represented as a function of temperature. In order to determine the temperature field, boundary conditions were introduced by setting a temperature value inside each of the process pipes, as shown in Fig. 9.

In order to allow thermal comparison between the supports in the L1–L3 transfer lines, the influence of thermal radiation was not included. The temperatures inside each of the process pipes were set in accordance with the values provided in Table 1. With the temperature field and heat flux densities in the whole model known, heat exchange paths between individual process pipes could be identified. The temperature field in the investigated model is shown in Fig. 10.

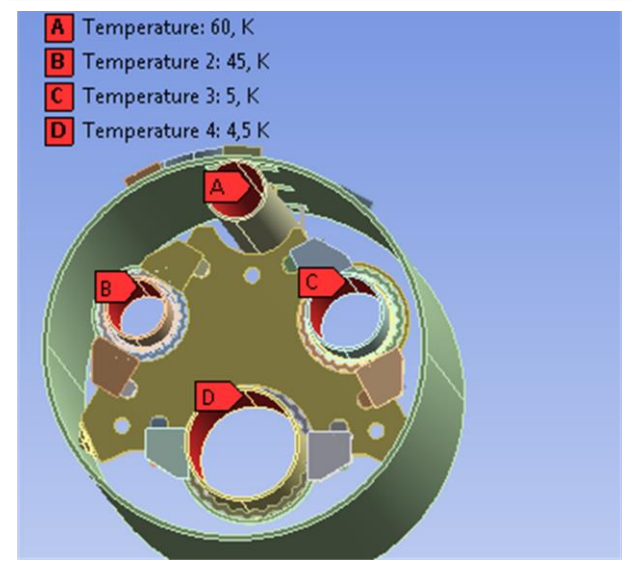


Fig. 9. Boundary conditions set for the process pipe sliding support in the L1 line.

In a similar way, the heat fluxes transferred to the process lines through strong and weak fixed supports were determined. Based on the general Eq. (5), its specific form was derived, which, utilizing the values of heat fluxes for individual process lines allows calculation the entropy fluxes generated in the transfer line by a given type of support:

$$\Sigma \dot{S} = n \sum_{i} \dot{S} = n \sum_{i} \frac{\dot{q}_{i}(T_{A} - T_{i})}{T_{i}^{2} \left(1 + \frac{T_{A} - T_{i}}{T_{i}}\right)},\tag{6}$$

where $\sum_i \dot{S}$ is the sum of entropy fluxes generated in process pipe due to heat flux, \dot{q}_i —heat flux to *i*-th the process pipe, and T_i is the temperature of *i* process pipe.

Table 2 includes the values of both heat fluxes and entropy fluxes.

The sliding support used in this model thermally connects pipes having a temperature of approximately 5 K with pipes for thermal shield cooling, which have temperatures of 45 K and 60 K. Such a connection results in heat flux in the location of the support, from the 45 K and 60 K pipes to the approx. 5 K pipes, causing negative entropy fluxes in the pipes for thermal shield cooling.

Using Eq. (4) and considering the flow and geometric parameters of the process pipes provided in Table1, the pressure losses and the corresponding fluxes of entropy generated for

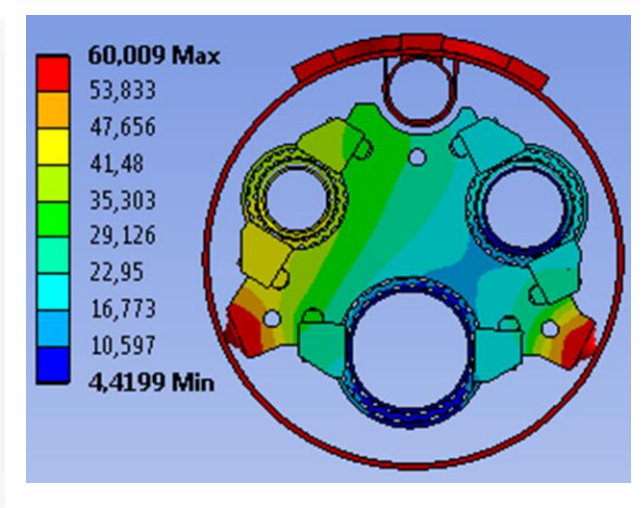


Fig. 10. Temperature field for the process pipe sliding support in the L1 line.

each process pipe were determined. As shown in Table 3, the entropy fluxes due to pressure losses relative to the entropy fluxes generated due to heat fluxes are negligibly low, so they will not be considered further.

Table 3. Pressure losses and the corresponding fluxes of entropy calculated for the L1 case.

-	K pply	4.5 K Return			5 K pply	60 K Return		ΣŚ _{Δρ} per
Δ <i>p</i> Pa	Ś _{Δρ} W/K	250m W/K						
14.3	0.000	11.0	0.002	167	0.002	230	0.003	0.007

5.2. Calculations of entropy fluxes generated in transfer line L2

In order to avoid any unwanted thermal contacts in the sliding supports of the L2 line, additional types of supports were introduced as shown in Figs. 8, 11 and 12.

Heat fluxes and the corresponding entropy fluxes for supports in the L2 transfer line were identified analogically to the procedure used in the sliding supports of the L1 transfer line. Figure 11 shows boundary conditions set for the thermal analysis of the supports. Figure 12 shows set temperature fields calculated for each type of the process pipe supports.

The results served to calculate values of heat fluxes through all supports to individual process pipes and the corresponding

Table 2. Heat fluxes to the process lines and the generated entropy fluxes calculated for the L1 case.

Type of	1	K pply		5 K turn		5 K ipply		50 K eturn	Pieces per	Pieces per	ΣŚΔ <i>T</i> , W/K
support	ġ, W	Ś _{Δτ} , W/K	<i>q</i> , W	Ś _{Δ7} , W/K	ġ, W	Ś _{Δτ} , W/K	ġ, W	<i>Ś</i> Δτ, W/K	12.5 m module	250 m segment	
Sliding	0.24	0.04	0.53	0.11	-0.19	0.00	-0.58	-0.01	4	80	11.5
Weak fix	0.04	0.01	0.06	0.01	0.01	0.00	22.90	0.31	1	20	6.5
Strong fix	0.17	0.03	0.31	0.06	0.10	0.00	7.02	0.09	1*	2	0.4

^{*}Strong fix support is only in the first and last module.

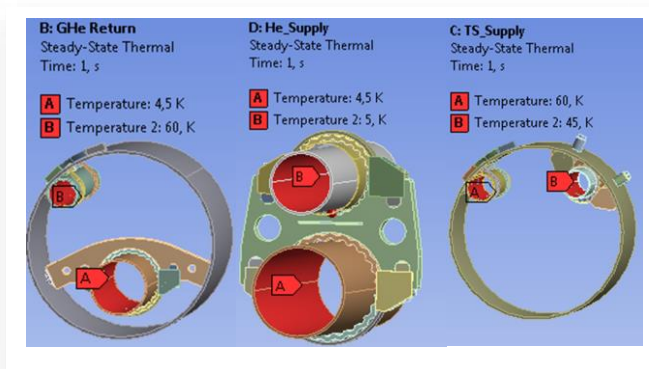


Fig. 11. Boundary conditions set for the process pipe sliding supports in the L2 line.

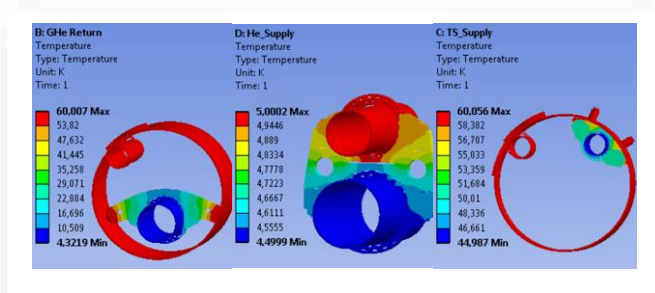


Fig. 12. Temperature fields calculated for the process pipe sliding supports in the L2 line.

entropy fluxes. Table 4 presents the results for all supports in line L2.

The sliding support system used in the L2 line significantly reduces heat fluxes to the supercritical helium supply line (5 K), as the pipe is thermally connected to the support pipe having a similar temperature. The heat leaks to the vapours return pipe (4.5 K) is likewise reduced, as the 45 K pipe is thermally connected directly to the thermal shield. Connecting the 45 K pipe directly to the thermal shield causes increased heat fluxes to this pipe. However, these heat leaks generate a smaller entropy flux than in the solution used for the L1 transfer line.

5.3. Calculations of entropy fluxes generated in transfer line L3

In the case of L3, where the process pipes are made of Invar, there is no necessity for the use of expansion joints. Consequently, there is also no justification for the application of light fixed supports to determine the axial and radial positioning of the process pipes at each of the expansion joints.

The sliding supports used in case L3 are identical to those in case L2. The number and position of sliding supports in case L2 is largely determined by the presence of compensation bellows. In case L3, where compensation bellows do not occur, the number and position of sliding supports is determined by the permissible value of the deflection arrow of the process pipes. For the purposes of this analysis, the permissible deflection arrow of the process pipes was assumed at 25×10^{-4} m. For the deflection arrow defined in this way, the distance between sliding supports should not exceed 3 m. The allowable distance between the individual sliding supports has been calculated on the basis of the following formula:

$$x = min \left| \sqrt[4]{\frac{87 f E(D_l^4 - d_l^4)}{20 g(\rho_{INV}(D_l^2 - d_l^2) + \rho_{He} d_l^2)}} \right|_i^1, \tag{7}$$

where f is the allowable value of process pipe deflection, E is the Young's modulus, D_i is the outside diameter of the i-th process pipe, d_i is the inside diameter of the i-th process pipe, ρ_{INV} is the Invar density, ρ_{He} is the density of helium transferred through the i-th process pipe, g is the acceleration of gravity.

The need to maintain a maximum distance of 3 m between sliding supports means that the number of sliding supports in the pipeline using process pipes made of Invar is the same as in the case of the L2 line. The difference between the support system for the L2 and L3 transfer lines is the absence of compensation bellows in the L3 line, which significantly reduces the entropy fluxes generated during the cryogen flow. Additionally, the most reliable transfer line is without bellows, which can be produced by using the Invar material [22]. Using a design without compensation bellows allows not only to limit heat leaks, but also to reduce the failure rate of the pipeline, as the bellows are the most failure-prone element of a cryogenic line [23]. Moreover, each compensation bellows requires an additional weld on the process pipe and the weld seam also becomes a potential failure spot. Although the probability of failure due to weld rapture is lower than the probability of compensation bellows rapture [24], reducing the number of welds has a significant role in reducing the failure rate of cryogenic transfer lines.

5.4. Summary of L1-L3 results

The application of second law of thermodynamic methods facilitates the optimization and characterization of cryogenic systems. Knowing the heat flows through the supports and the entropy fluxes generated as a result of them for each of the analysed cases of transfer lines from Eq. (1), one can determine the additional

Table 4. Heat fluxes to the process pipes and the generated entropy fluxes calculated for the sliding support system of the L2 transfer line (data provided for one support of each type).

Type of sup- port		5 K ipply		5 K turn		I5 K ipply		60 K eturn	Pieces per 12.5 m	Pieces per 250 m	ΣĆ
	ġ, W	Š _{Δτ} , W/K	ġ, W	<i>Ś</i> Δτ, W/K	ġ, W	Ś _{Δτ} , W/K	ġ, W	<i>Ś</i> Δτ, W/K	module	segment	ΣŠ _{Δτ} , W/K
Sliding	0.00	0.00	0.45	0.09	0.38	0.00	-0.83	-0.01	4	80	6.7
Weak fix	0.04	0.01	0.06	0.01	0.01	0.00	22.9	0.31	1	20	6.5
Strong fix	0.17	0.03	0.31	0.06	0.10	0.00	7.02	0.09	1*	2	0.4

^{*}Strong fix support is only in the first and last module.

Table 5. The summary of the generated entropy fluxes and theoretical and real additional power for each analysed pipeline case.

	5 Κ Supply ŚΔτ, W/Κ	4.5 K Return ŚΔτ, W/K	45 K Inlet Ś _{Δτ} , W/K	60 K Outlet ŚΔτ, W/K	ΣŚ _{Δ7} , W/K	<i>Р_{АdT},</i> W	P _{AdR} , kW
L1	3.74	9.09	-0.08	5.66	18.41	5431	18.10
L2	0.20	7.77	0.17	5.40	13.54	3994	13.31
L3	0.04	7.53	0.17	-0.69	7.04	2112	6.92

 P_{AdT} and P_{AdR} are the theoretical and real additional power required to overcome irreversibilities associated with heat leaks during pipeline flow ($P_{AdR} = P_{AdT}/0.3$).

power necessary to overcome the irreversibilities accompanying the flow [25,26]. In order to determine the actual additional power required to overcome the described irreversibilities, it is necessary to take into account the thermodynamic efficiency of the cryogenic refrigerator, which, as indicated in Section 1, is 0.3 Carnot efficiency. Table 5 presents a summary of the generated entropy fluxes and theoretical and real additional power for each analysed pipeline case.

6. Conclusions

The results for the 250 m segments of the L1, L2 and L3 design type transfer lines demonstrate that the use of new sliding supports system shown in the L2 and L3 design significantly reduces the additional power which would need to be supplied to the condensing unit if only one type of sliding support was used for all process pipes. The obtained results indicate also that using cryogenic transfer lines with Invar process pipes rather than stainless steel pipes reduces the number of supports present in the transfer line and limits the entropy fluxes generated during the flow. It is proved that transfer line using Invar process pipes to be the best solution from a thermodynamic point of view and allows reduction the operating costs of the studied multichannel cryogenic transfer line by more than 2.5 times. This study shows that using cryogenic transfer lines comprising Invar process pipes offer the possibility to significantly improve thermodynamic parameters and at the same time to increase the mechanical stability of the pipeline, as no compensation bellows need to be used in the process pipes.

The use of the process pipes made of Invar in cryogenic transfer lines is currently very rare, because the cost of Invar pipes themselves is very high, which significantly increases the installation costs. However, in the case of long installations, as is the case for the Future Circular Collider accelerator, it is possible to purchase large series of Invar pipes, which significantly reduces the investment costs. Taking into account the results of this analysis, it can be stated that in the case of appropriately long installations, it is reasonable to use Invar process pipes, which reduce operating costs and increase the reliability of the pipeline.

Based on the performed analysis it can be concluded that an optimization approach based on the use of the second law of thermodynamics and Gouy-Stodola theory allows a comprehensive assessment of the thermodynamic efficiency of systems, in which there is a mass flow of fluids with different thermody-

namic parameters. Entropy in this case plays the role of a common denominator, which can be easily converted into the additional power required to be supplied to the device to compensate the effects of irreversibility. The presented method can therefore be used for complex optimization taking into account thermal, flow and design parameters of entire distribution systems, as well as their individual components such as transfer lines, valve boxes or execution modules.

Acknowledgements

The work has been supported by the National Centre of Nuclear Research at Warsaw in the framework of Polish in-kind contribution to the construction of the European Free Electron Laser XFEL and by CERN at Geneva in the framework of conceptual design of Future Circular Collider cryogenic system.

References

- [1] Deng, B.C., Yang, S.Q., Xie, X.J., Wang, Y.L., Pan, W., Li, Q., & Gong, L.H. (2019). Thermal performance assessment of cryogenic transfer line with support and multilayer insulation for cryogenic fluid. *Applied Energy*, 250, 895–903. doi: 10.1016/j. apenergy.2019.05.025
- [2] Rohan, D., Ghosh, P., & Chowdhury, K. (2011). Application of parallel heat exchangers in helium refrigerators for mitigating effects of pulsed load from fusion devices. *Fusion Engineering and Design*, 86(4-5), 296–306. doi: 10.1016/j.fusengdes.2011.01.133
- [3] Iwamoto, A., Nobutoki, M., Kumaki, T., Higaki, H., Hamaguchi, S., Takahata, K., Imagawa, S., Mito, T., Takada, S., & Nadehara, K. (2017). In-situ calibration method of orifice flow meter equipped in 600 W helium refrigerator/liquefier with variable temperature supplies. Fusion Engineering and Design, 123, 107–110. doi: 10.1016/j.fusengdes.2017.05.045
- [4] Benedikt, M., & Zimmermann, F. (2016). Status of the Future Circular Collider Study. 25th Russian Particle Accelerator Conference, 21-25 Nov., Saint Petersburg, Russia, TUYMH01. doi: 10.18429/JACoW-RuPAC2016-TUYMH01
- [5] Collier, P. (2015). The technical challenges of the Large Hadron Collider. Philosophical Transactions A: Mathematical, Physical and Engineering Sciences, 373, 20140044. doi: 10.1098/rsta. 2014.0044
- [6] Gistau-Baguer, G. (2020). Cryogenic Helium Refrigeration for Middle and Large Powers. In International Cryogenics Monograph Series, Weisend II, J.G., Jeong, S. (eds.). Springer Nature Switzerland AG. doi: 10.1007/978-3-030-51677-2
- [7] Quack, H.H. (1994). Maximum efficiency of helium refrigeration cycles using non-ideal components. In Advances in Cryogenic Engineering, vol. 39, Kittel, P. (ed.). Springer, Boston, MA. doi: 10.1007/978-1-4615-2522-6 148
- [8] Van Sciver, S.W. (2012). Helium Cryogenics (1st ed.). In

- International Cryogenics Monograph Series, Timmerhause K.D., Rizzuto, C. (eds.). Springer. doi: 10.1007/978-1-4419-9979-5
- [9] Chorowski, M., Choudhury, A., Datta, T.S., & Polinski, J. (2008). Synthesis of the multilayer cryogenic insulation modeling and measurments. AIP Conference Proceedings, 985(1), 1367–1374. doi: 10.1063/1.2908496
- [10] Khan, M.N., Ahmad, S., Wang, Z., Hussien, M., Alhuthali, A.M.S., & Ghazwani, H.A. (2024). Flow and heat transfer insights into a chemically reactive micropolar Williamson ternary hybrid nanofluid with cross-diffusion theory. *Nanotechnology Reviews*, 13(1), 20240081. doi: 10.1515/ntrev-2024-0081
- [11] Khan, M.N., Ahmad, S., Wang, Z, Ahammad, N.A., & Elkotb, M.A. (2023). Bioconvective surface-catalyzed Casson hybrid nanofluid flow analysis by using thermodynamics heat transfer law on a vertical cone. *Tribology International*, 188, 108859. doi: 10.1016/j.triboint.2023.108859
- [12] Mohanty, B., Mohanty, S., Mishra, S.R., & Pattnaik, P.K. (2021). Analysis of entropy on the peristaltic transport of micropolar nanofluid: a simulation obtained using approximate analytical technique. *The European Physical Journal Plus*, 136, 1139. doi: 10.1140/epjp/s13360-021-02150-z
- [13] Nadeem, S., Ishtiaq, B., Akkurt, N., & Ghazwani, H.A. (2023). Entropy optimized flow of hybrid nanofluid with partial slip boundary effects and induced magnetic field. *International Journal of Modern Physics B*, 37(29), 2350252. doi:10.1142/s0217979223502521
- [14] Bejan, A. (1980). Second law analysis in heat transfer. *Energy*, 5(8-9), 712–732. doi: 10.1016/0360-5442(80)90091-2
- [15] Mahmud, S., & Fraser, R.A. (2002). Second law analysis of the heat transfer and fluid flow inside a cylindrical annular space. *Exergy an International Journal*, 2(4), 322–329. doi: 10.1016/ S1164-0235(02)00078-X
- [16] Bejan, A. (1995). Entropy Generation Minimization. The Method of Thermodynamic Optimization of Finite-Size Systems and Finite-Time Processes. CRC Press. doi: 10.1201/9781482239171
- [17] Pietsch, M., Rummel, T., Nagel, M., Bosch, H.S.F., & Carovani, F. (2023). Development, design and installation of multichannel transfer lines at W7-X under extreme geometrical constraints. Fusion Engineering and Design, 188, 113429. doi: 10.1016/j.

- fusengdes.2023.113429
- [18] Duda, P., Chorowski, M., & Polinski, J. (2017). Impact of process parameters and design options on heat leaks of straight cryogenic distribution lines. *Physical Review Accelerators and Beams*, 20, 033202. doi: 10.1103/PhysRevAccelBeams.20.033202
- [19] Duda, P., Chorowski, M., & Polinski, J. (2020). Entropy analysis of support systems in multi-channel cryogenic lines. *IOP Conference Series: Materials Science and Engineering*, 755, 012065. doi: 10.1088/1757-899X/755/1/012065
- [20] Rusiński, E., Chorowski, M., Iluk, A., Fydrych, J., & Malcher, K. (2014). Selected aspects related to the calculations and design of a cryogenic transfer line. *Archives of Civil and Mechanical Engineering*, 14(2), 231–241. doi: 10.1016/j.acme.2013.11.003
- [21] Chuang, P.-S., Chang, S.-H., Chiou, W.-S., Hsiao, F.-Z., Li, H.-C., Liao, W., Lin, T.-F., & Tsai, H. (2016). Development of multi-channel line for the NSRRC cryogenic system. 7th International Particle Accelerator Conference, 8-13 May, Busan, Korea, doi: 10.18429/JACoW-IPAC2016-TUPMB050
- [22] Thakkar, A., & Vyas, M.I. (2011). Design & analysis of bellows free cryogenic transfer line. 2nd International Conference on Current Trends in Technology 'NUiCONE-2011', 8-10 Dec., Ahmedabad, India.
- [23] Cadwallader, L.C. (2010). Vacuum bellows, vacuum piping, cryogenic break and copper joint failure rate estimates for ITER design use. Idaho National Laboratory, INL/EXT-10-18973, USA. doi: 10.2172/983360
- [24] Cadwallader, L.C. (1992). Cryogenic system operating review for fusion application. Idaho National Engineering Laboratory, Technical Raport, EGG-FSP-10048, ON: DE92012509, USA. doi: 10.2172/5550141
- [25] Kirkconnell, C.S., & Curran, D.G.T. (2002). Thermodynamic optimization of multi-stage cryogenic systems. AIP Conference Proceedings, 613(1), 1123–1132. DOI: 10.1063/1.1472137
- [26] Hånde, R., & Wilhelmsen, Ø. (2019). Minimum entropy generation in a heat exchanger in the cryogenic part of the hydrogen liquefaction process: On the validity of equipartition and disappearance of the highway. *International Journal of Hydrogen Energy*, 44(29), 15045–15055. doi: 10.1016/j. ijhydene.2019.03.229